The 2013 World Congress on
Advances in Structural Engineering and Mechanics (ASEM13)
Jeju, Korea, September 8-12, 2013

A Modal Displacement Based approach for the Seismic Design of one way asymmetric multi story buildings

Philip J. Wilkinson[1], *Oren Lavan[2]

Technion – Israel Institute of Technology
Technion City, Haifa 32000, Israel
[1] phil@tx.technion.ac.il
[2] lavan@tx.technion.ac.il

ABSTRACT

This paper presents the extension of the new Modal Displacement Based seismic Design methodology to multistory one way asymmetric plan Reinforced Concrete (RC) wall structures considering unidirectional ground motion. The methodology accounts for the unique characteristics of the specific building layout. The influence of ductility and dynamic higher mode effects are considered explicitly and directly in the design process. As a result, empirical factors based on parametric studies are not required nor is a traditional capacity design phase. Rather, capacity design principles are incorporated at the beginning of the design procedure when the design engineer specifies a desired distribution of relative flexural strength. In this paper, axial loads on walls are taken into account when specifying the relative strength distribution. This improves the methodology's ability to achieve a desired reinforcing steel distribution. Like the DDBD method, the proposed methodology relies on a strong theoretical basis and makes use of simplified tools so can easily be used in practical design.

1. INTRODUCTION

The nonlinear response of ductile irregular structures is much harder to predict than the response of ductile regular structures. *Design* procedures for the later class of structure have been the subject of much research effort over the last few decades. These design methodologies are now well developed and are starting to be included in seismic design codes around the world.

Nonlinear *analysis* methods (e.g. nonlinear static and dynamic procedures) are now generally accepted by seismic codes for the purpose of *verification*. It is also well known that the response of irregular buildings is significantly affected by higher mode effects. Hence, verifications for design of ductile irregular structures should, preferably, be done using nonlinear dynamic procedures (e.g. Nonlinear Time History Analysis – NTHA, Modal Pushover Analysis – MPA (Chopra and Goel, 2002), or Effective Modal Superposition – EMS (Kowalsky, 2002 and Alvarez, 2004)).

Practical and reliable seismic *design* methods, such as Direct Displacement Based Design (DDBD) (Priestley, Calvi and Kowalsky, 2007), are now readily available for regular buildings and slightly irregular buildings having minimal strength eccentricity and significant ductility demands. However, developing a practical design methodology which can reliably endow generally irregular structures with the ability to achieve target performance levels remains an ongoing challenge for the earthquake engineering community. Design methods for irregular buildings for ductile response must consider both nonlinear and dynamic (i.e. multi-modal) effects. Such a method, called Modal Displacement Based Design (MDBD), has been proposed by Wilkinson, Lavan and Rutenberg (2012) for *single story* one way asymmetric plan RC wall structures subjected to unidirectional ground motions.

MDBD was extended in Wilkinson and Lavan (2013) to multistory one way asymmetric plan RC wall structures subjected to unidirectional ground motion. This extension involved shifting the focus of the design procedures from a single „global' response measure for each wall to local wall responses at each floor level and within each story. In addition, capacity design concepts were included in the process and geometric nonlinearity effects had to be accounted for.

In this paper that extension is completed by including explicit consideration of the contribution of gravity axial loads to the wall moment capacities in the process of specifying the relative flexural strength distribution. This improves the methodology's ability to realise any desirable reinforcing steel distribution in the final design.

These new considerations necessitated some modifications to the design methodology as proposed in the earlier papers. MPD and DMPD designs of a torsionally restrained (Castillo, 2004) eight story mass eccentric one way asymmetric plan RC wall structure are carried out and verified using NTHA with 20 historic ground motions scaled to a selected design response spectrum. The results are discussed and conclusions drawn.

2. PROBLEM STATEMENT

A situation which often occurs in practice was selected as the starting point for the design procedures. It was assumed that the seismic engineer receives architectural building plans showing the sizes and locations of the walls. The structural geometry is therefore taken as predetermined. The design code specifies the seismic intensity at the building site location for each limit state. The seismic demand is generally presented in the form of a 5% damped elastic response spectrum (RS).

Both MPD and DMPD currently use inelastic constant ductility RS for bi-linear hysteresis rules having any post-yield stiffness reduction factor. Methods have been proposed for converting a 5% damped elastic response spectrum to an inelastic constant ductility RS for any bi-linear hysteresis rule (see e.g. refs. in Chopra, 2007).

The target performance levels for each limit state are defined by the code in the form of maximum acceptable values for selected response parameters. Typically these parameters include interstory drifts and material strains limits.

The equation governing the nonlinear response of a multistory RC wall building to a unidirectional ground motion is shown as Eq. (1):

$$\mathbf{M}\ddot{\boldsymbol{u}}(t)+\mathbf{C}\dot{\boldsymbol{u}}(t)+\mathbf{F_s}(\boldsymbol{u},\dot{\boldsymbol{u}})=-\mathbf{M}\boldsymbol{l}\ddot{u}_g(t) \tag{1}$$

where **M** and **C** are the mass and damping matrices respectively, $\boldsymbol{u}(t)$ is the displacement vector relative to the ground in global coordinates and the overdots denote the order of the derivatives with respect to time, *t*. ***l*** is the influence vector describing rigid body motion corresponding to a unit ground displacement in the direction of the excitation and $\ddot{u}_g(t)$ is the ground acceleration which expresses the seismic demand. $\mathbf{F_s}(\boldsymbol{u}, \dot{\boldsymbol{u}})$ represents the forces generated by the walls as they resist deformation.

Examining the terms in Eq. (1) shows how the seismic engineer can influence the response of a structure to a given ground motion. **M** is essentially fixed by the building geometry and the construction materials. $\ddot{u}_g(t)$ expresses the seismicity specified by the code and $\mathbf{C}$ is typically taken as a function of **M** and the structure's initial elastic stiffness **K**. For each limit state, the code specifies limits on response parameters directly related to $\boldsymbol{u}$ and sometimes also on total accelerations.

If no supplemental energy dissipating devices are included in the design, then only $\mathbf{F_s}(\boldsymbol{u}, \dot{\boldsymbol{u}})$ remains to be engineered. An elastic perfectly plastic (EPP) approximation to the actual hysteretic behavior of a RC element may not be 100% accurate. Nevertheless, it is more realistic to employ EPP models at the plastic hinge level than to use an elastic model coupled with the equal displacement approximation, which is what most existing force-based design methods use.

The stiffness of a RC Lateral Load Resisting Element (LLRE), such as a RC structural wall, can be defined as a function of the element's flexural strength by using the well-known beam equation relating curvature, $\boldsymbol{\phi}$**,** to moment demand, $\boldsymbol{M}$**,** and flexural stiffness, $\boldsymbol{EI}$**,** as shown in Eq. (2)

$$\boldsymbol{\phi} = \boldsymbol{M}/\boldsymbol{EI} \tag{2}$$

An EPP approximation of the $\boldsymbol{M} - \boldsymbol{\phi}$ response of any element section may be developed using validated estimates of the nominal yield curvature and yield moment. The initial elastic branch of the bilinear approximation can represent elastic section stiffness to nominal yield. $\boldsymbol{EI}$ is therefore computed as $\boldsymbol{EI} = \boldsymbol{M_y}/\boldsymbol{\phi_y}$. Estimates of $\boldsymbol{\phi_y}$ typically depend only on the yield strain of the longitudinal reinforcing steel and the element geometry. For RC walls having rectangular cross sections $\boldsymbol{\phi_y} = \boldsymbol{2\epsilon_{sy}}/\boldsymbol{l_w}$ is often used.

The nominal yield moment of a RC wall having a rectangular cross section depends on the steel reinforcing ratio, the wall cross section geometry and the axial load. As the wall lengths are taken as predetermined and the axial forces can be estimated with reasonable accuracy, only ρ remains to be determined by the engineer.

The design problem can then be stated as follows: Given the geometry of a multistory RC wall building and the design seismic intensity and target performance levels for each applicable limit state, determine acceptable values of the longitudinal steel reinforcing ratios, $\rho_{j,i}$ for all walls $i = 1{:}\,N_w$ and all stories $j = 1{:}\,N_s$, which enable the structure to achieve, as near as possible, the target performance levels for the governing limit state.

3. SOLUTION SCHEME: MDBD for One Way Asymmetric Plan Wall Structures

3.1. Design for linear response.

It is well known (see e.g. Chopra, 2007) that the maximum elastic displacement, $\boldsymbol{u_m}$**,** of a structure to an earthquake ground motion can be estimated as a combination of modal contributions, $\boldsymbol{u_{mn}}$. In many cases, the square root of the sum of the squares (SRSS) combination rule can be applied. If applied to the term $\boldsymbol{\phi_{jn}}$ for the jth story for the nth mode one obtains:

$$\boldsymbol{u_{mj}} = \sqrt{\sum_{n=1}^{N}(\boldsymbol{u_{mjn}}^2)} = \sqrt{\sum_{n=1}^{N}(\Gamma_n \boldsymbol{\phi_{jn}} D_n)^2} \tag{4}$$

where $\Gamma_n = L_n/M_n$ where $L_n = \boldsymbol{\phi}_{\boldsymbol{n}}^T\mathbf{M}\boldsymbol{l}$ and $M_n = \boldsymbol{\phi}_{\boldsymbol{n}}^T\mathbf{M}\boldsymbol{\phi_n}$ where $\boldsymbol{\phi_n}$ is the nth mode shape. D_n is the nth mode spectral displacement.

Defining $\gamma_{Dn} = D_n/D_1$ and $u_{lmn,cr} = \boldsymbol{a_{w,cr}}\boldsymbol{u_{mn}}$ where $u_{lmn,cr}$ is the nth mode's contribution to the allowable displacement $u_{lm,cr}$ (corresponding to the design code deformation limit state) of the critical wall, in its local coordinates, and $\boldsymbol{a_{w,cr}}$ is a global to local coordinate transformation matrix for the critical wall. In this paper interstory drifts are limited to 2% and longitudinal reinforcing steel strains are limited to $40\varepsilon_{sy}$. This approximates a damage control limit state. Eq. (4) is shown for displacements however it is easily adjusted for computation of drifts. Eq. (4) may be rearranged to obtain D_1 as a function of γ_{Dn}, $u_{lm,cr}$, Γ_n and the mode shapes $\boldsymbol{\phi_n}$ as

$$D_1 = \frac{u_{lm,cr}}{\sqrt{\sum_{n=1}^{N}\left(\boldsymbol{a_{w,cr}}\Gamma_n\boldsymbol{\phi_n}\gamma_{Dn}\right)^2}} \tag{5}$$

Eq. (5) may be used to compute the design spectral displacement for a SDF substitute structure representing 1st mode response for a displacement-based design procedure for linear response which directly considers higher mode response. Only the ***relative*** wall stiffnesses are required for computing the mode shapes and relative periods. The ratios between the relative periods are used to compute γ_{Dn}.

3.2. Design for nonlinear response.

Eq. (5) can also be used in design for nonlinear response. This is applicable only when the approximation (additional to that of estimating peak seismic responses using modal combination rules) inherent in neglecting the modal coupling due to yielding is acceptable (Chopra and Goel, 2002). In the nonlinear case D_1 may be determined iteratively from inelastic constant ductility design spectra or an elastic design spectrum using R-μ-T relationships (see e.g. refs. in Chopra, 2007) or estimated directly using „effective mode' shapes as presented in the step-by-step outline for the DMPD procedure below.

3.3. Overview of MDBD procedures

MDBD currently consists of two similar but independent design procedures. Both use constant ductility response spectra and involve modal pushover analysis of multi-degree of freedom (MDF) models. The first procedure, called Modal Pushover Design (MPD) is an „inverse MPA' procedure and is iterative at the single degree of freedom (SDF) level. MPD achieves the target performance level exactly when verified using Modal Pushover Analysis (MPA). The second procedure, called Direct Modal Pushover Design (DMPD) is direct not iterative, and involves computing „effective' modes characterized by plastic hinge secant rotational stiffnesses corresponding to an estimated peak displacement profile. Both design procedures are applied in the context of a given structural geometry, set of material properties and design code limit states.

Similarly to DDBD, yield and limit displacements of all walls are estimated from material and section properties and element curvature distributions. A relative strength distribution is then chosen by the design engineer and relative elastic stiffnesses, to nominal yield, are computed. In DMPD secant plastic hinge stiffnesses, to peak ductility, are also estimated and effective „modes' computed to estimate the relative „modal' contributions at peak response. Modal pushover curves are used to define the yield displacement of a nonlinear SDF system for each mode.

The fundamental period T_1 corresponding to the critical location achieving its deformation limit is computed iteratively in MPD and estimated directly in DMPD. The total response at each location, including all significant „modal' contributions, is set equal to that location's limit deformation. The limit deformation of each location corresponds to a unique c_M displacement through the „modes'. The minimum of these c_M displacements is associated with the critical location's limit deformation. This minimum c_M displacement is used (implicitly) in Eq. (5) to define the design 1st mode spectral displacement D_1. T_1 can then be retrieved from the constant ductility RS using D_1 and μ_1. Once T_1 is known the design moments and shears can be computed. The design actions can then be used to perform section design following standard code procedures.

3.4. MDBD step-by-step procedure outlines

<u>3.4.1. Modal Displacement Based Design: Step-by-step procedure outline</u> The MPD and DMPD procedures are identical except for step 10.

1) Obtain the structure's geometry and material properties.

2) Select a limit state which is likely to govern the design.
   a) Define design site seismicity in the form of constant ductility RS.
   b) Define target performance levels in the form of limits on interstory drifts and material strains.
   c) Compute seismic floor masses for the considered load case.

3) Estimate yield and limit deformations.

4) Specify the distribution of relative flexural strength.

5) Compute relative elastic wall flexural stiffnesses to nominal yield.

6) Compute modal characteristics using relative stiffnesses.

7) Conduct modal pushover analyses.

8) Approximate the pushover curves bilinearly.

9) Define an equivalent nonlinear SDF system for each significant mode.

10) Determine the value of T_1 which corresponds to the critical location achieving its limit deformation.

11) Scale strengths and stiffnesses to match the design T_1.

12) Compute design moments considering geometrical nonlinearity (PΔ effects).

13) Compute design shears considering geometrical nonlinearity (PΔ effects).

14) Repeat steps 2-13 for all other relevant limit states which may govern the design

<u>3.4.2. Modal Displacement Based Design: Detailed step-by-step procedure</u> The procedure is first presented in full for Modal Pushover Design. Steps 1-9 and 11-14 are identical for both procedures. Step 10 for Direct MPD is presented after step 14.

1) Obtain the structure's geometry and material properties.

The geometry includes the wall locations and dimensions and design steel and concrete strengths.

2) Select a limit state which is likely to govern the design.

a) The seismicity is defined by the design constant μ displacement RS for the site. Typically design codes provide 5% damped elastic pseudo acceleration RS. This is usually modified to account for the limit state considered, the structure's importance and the site's relative seismicity and soil conditions.

As the pushover curves are approximated bilinearly, constant ductility displacement RS, $D(r, \mu, T)$, for bilinear hysteretic behavior are required. Krawinkler and Nassar (1992) proposed formulae for computing such RS approximately from an elastic displacement RS. Alternatively, $D_n(r_n, \mu_n, T_n)$ may be computed by NTHA of the equivalent bilinear SDF system for the n^{th} mode using an appropriate set of ground motions scaled to match the design seismicity for the limit state considered.

b) Performance targets are typically defined by code interstory drift and material strain limits. Typical drift limits are 1% and 2% for serviceability and damage control limit states respectively.

For a serviceability limit state Priestley et al (2007) recommended limits on concrete and steel material strains of $\epsilon_{c,ls} = 0.004$ and $\epsilon_{s,ls} = 0.015$ respectively. For a damage control limit state the recommended limits on concrete and steel material strains are $\epsilon_{c,ls} = 0.018$ and $\epsilon_{s,ls} = 0.6\epsilon_{su}$ (where ϵ_{su} is the steel strain at peak steel stress) respectively.

These damage control limit state strain values for RC walls were determined assuming sufficient transverse reinforcing steel to provide enough confinement to the concrete and longitudinal reinforcing steel in compression areas to enable the concrete to achieve an ultimate compression strain of 0.018. Priestley et al (2007) suggested that these damage control strain limits for RC walls may be used for concrete strengths in the range $15MPa \leq f_c' \leq 35MPa$ and design steel yield stresses in the range $270MPa \leq f_y \leq 500MPa$.

c) Compute seismic floor masses. This may depend on the particular load case and limit state being considered.

3) Estimate yield and limit deformations.

Estimate the following deformation parameters using appropriate code equations. In lieu of code equations the following recommendations from Priestley et al (2007) may be used:

Yield curvatures, φ_{yi} for walls with rectangular cross sections:

$$\varphi_{yi} = \frac{2\epsilon_{sy}}{L_i} \tag{6}$$

where ϵ_{sy} is the longitudinal reinforcing steel yield strain and L_i is the length of the i^{th} wall.

Strain based curvature limits, φ_{lsi}, for all intended plastic hinge regions:

The curvatures corresponding to the material limit strains selected in step 2b) are estimated for RC walls, for both limit states, as

$$\varphi_{lsi} = \frac{1.2\epsilon_{s,ls}}{L_i} \tag{7}$$

Plastic hinge lengths:

$$L_{pi} = kh_{ei} + 0.1L_i + L_{SP} \tag{8}$$

where $k = 0.2(f_u/f_y - 1) \leq 0.08$ where f_u is the ultimate steel stress and $h_{ei} = 0.75h_r$ where h_r is the roof height. L_{SP} is the strain penetration length computed by $L_{SP} = 0.022f_y d_{bl}$ where d_{bl} is a reasonable estimate of the diameter of the longitudinal reinforcing steel.

Allowable plastic hinge rotations:

$$\theta_{p,i} = \min\left[\left(\varphi_{lsi} - \varphi_{yi}\right)L_{pi},\ \theta_{lim} - \theta_{ry,i}\right] \geq 0 \tag{9}$$

where θ_{lim} is the drift limit for the selected limit state and $\theta_{ry,i} = 0.5h_r\varphi_{yi}$ is the yield drift of the i^{th} wall at the roof level.

4) Specify the distribution of relative flexural strength.

The lateral distribution of flexural strength defines the strength eccentricity e_V. The lateral and vertical distributions of flexural strength should comply with capacity design principles in order to restrict yielding to the intended plastic hinge regions

(PHRs). Selection of vertical distribution of flexural strength may be influenced by code capacity envelope requirements.

The strength distribution may be defined as the relative nominal yield moment capacities, $M'_{yj,i}$, of the jth region (or story) of the ith wall. Initially the distribution of flexural strength up each wall may be expressed as factors of the base moment capacity of each wall such that $M'_{y1,i} = 1$ for all i. The absolute values of the moment capacities due to axial loads are known approximately. Neglecting eccentricity in these axial loads, the base moment capacity of each wall may be estimated assuming a reasonable longitudinal steel reinforcing ratio of, say, $\rho'_{1,i} = 0.01$ using Eq. (10) for RC walls:

$$M'_{y1,i} = \xi_i \, \rho'_{1,i} L_i^2 + \alpha L_i N_{1,i} \tag{10}$$

where $\xi_i = \alpha f_y b_i$ where b_i and L_i are the i^{th} wall's thickness and length respectively, and f_y is the design yield strength of the longitudinal reinforcing steel. α is a constant (≈ 0.45) which depends on section properties for relatively low levels of axial load ($N_{j,i} < 0.2 f_c' A_{gi}$) and $N_{j,i}$ is the design axial force in the jth region (or story) of the ith wall for the selected load case and limit state.

The flexural strength distribution may then be pre-scaled by multiplying the distribution for each wall, $M'_{yj,i}$ for $j = 2{:}\, N_s$ (where N_s is the number of stories in the building), by $M'_{y1,i}$. This defines the target distribution of flexural strength accounting for the effects of axial loads on the horizontal distribution (between walls) of flexural strength. Some design codes specify the shape of wall moment capacity envelopes. If so, this may need to be respected in selecting the vertical flexural strength distribution.

The relative lateral strength distribution resulting from the process above is based on a reinforcing steel distribution $\rho'_{j,i}$ in which all walls in the same direction have similar reinforcing ratios in each story. Alternatively, the lateral distribution of strength could be based on a target strength eccentricity e_V, possibly with the aim of optimizing the seismic design.

5) Compute relative elastic wall flexural stiffnesses to nominal yield.

$$EI'_{j,i} = M'_{yj,i} / \varphi_{yi} \tag{11}$$

6) Compute modal characteristics using relative stiffnesses.

Compute elastic mode shapes of free vibration $\boldsymbol{\phi}_\mathbf{n}$ by forming the global stiffness and mass matrices and using an eigenvalue solver. Alternatively a finite element model of the MDF structure could be built in a structural analysis program capable of computing mode shapes and modeling nonlinear material force-deformation response (flexural yielding). Use the known wall geometry and material properties and the relative flexural stiffnesses, $EI'_{j,i}$, and strengths $M'_{yj,i}$ to characterize the structure.

Normalize the mode shapes by the roof c_M translational term. Compute the relative frequencies ω_n', relative periods T_n' and the ratios between the relative periods $\gamma_{Tn} = T'_n/T'_1$. Compute the modal participation factors $\Gamma_n = L^h_n/M_n$ where $L^h_n = \boldsymbol{\phi}^{\mathrm{T}}_{\mathbf{n}}\boldsymbol{M}\boldsymbol{l}$ where $\boldsymbol{M}$ is the diagonal mass matrix and $\boldsymbol{l} = \begin{Bmatrix}\widehat{\mathbf{1}}\\ \widehat{\mathbf{0}}\end{Bmatrix}$ where $\widehat{\mathbf{1}}$ and $\widehat{\mathbf{0}}$ are column vectors of ones and zeros respectively each of order N_s where N_s is the number of stories. $M_n = \boldsymbol{\phi}^{\mathrm{T}}_{\mathbf{n}}\boldsymbol{M}\boldsymbol{\phi}_{\mathbf{n}}$. Compute the modal effective masses $m_n = \Gamma^2_n M_n$ and heights $h_n = L^\theta_n/L^h_n$ where $L^\theta_n = \boldsymbol{h}\boldsymbol{M}_{\boldsymbol{N_s}}\boldsymbol{\phi}_{\mathbf{n},\boldsymbol{N_s}}$ where $\boldsymbol{h}$ is a row vector of order N_s containing the floor heights in ascending order, $\boldsymbol{M}_{\boldsymbol{N_s}}$ is the diagonal N_s by N_s submatrix of $\boldsymbol{M}$ containing the floor translational masses and $\boldsymbol{\phi}_{\mathbf{n},\boldsymbol{N_s}}$ is a column vector of order $\boldsymbol{N_s}$ containing the terms of $\boldsymbol{\phi}_{\mathbf{n}}$ corresponding to the floor translational degrees of freedom.

Exclude all insignificant modes. Most codes allow this to be done on the basis of the 1st N_m modal effective masses summing to at least 90% of the total seismic mass of the building.

7) **Conduct Modal Pushover Analyses.**

Develop modal base shear – reference displacement ($V'_{bn} - u_{rn}$) curves by conducting N_m (one for each mode contributing significantly to the total response) pushover analyses on an MDF structural model. Neglect geometric nonlinearity. For each pushover analysis apply a unique invariant load vector defined as

$$\boldsymbol{p_n} = \mathbf{M}\boldsymbol{\phi_n} \tag{12}$$

It was found that the best reference node location was in line with the centers of mass at the modal effective height, h_n. This could be because this is where the resultant of the applied lateral loads act. At each load increment, record global and local responses of interest including the translations and rotations of all floors at the center of mass, interstory drifts at critical locations like the floor slab edges and wall curvatures, moments and shears.

8) **Approximate the pushover curves bilinearly** without changing the initial elastic stiffness, k_{eln}, by defining the relative yield shear V'_{yn} and a post yield - elastic stiffness ratio r_n. V'_{yn} and r_n can be computed by equating the area under the bilinear approximation to the known area under the pushover curve from $u_{rn} = 0\ to\ u_{endn}$ where u_{endn} is the translation of the reference node at a selected point, for example, the end of the pushover analysis. The area under the bilinear approximation can be formulated as a function of u_{yn} which is the reference node translation at nominal yield of the MDF system. $V'_{yn} = k_{in}u_{yn}$ and $r_n = k_{inn}/k_{eln}$ where $k_{inn} = (V'_{endn} - V'_{yn})/(u_{endn} - u_{yn})$ where V'_{endn} is the base shear at $u_{rn} = u_{endn}$.

9) **Define an equivalent nonlinear SDF system for each significant mode** having the same yield shear and post yield - elastic stiffness ratio as defined for the

bilinear approximation of the MDF system pushover curve and the spectral yield displacement defined by Eq. (13):

$$D_{yn} = \frac{V'_{yn}}{{\omega'_n}^2 m_n} \tag{13}$$

10) Iteratively determine the $\mathbf{T_1}$ corresponding to the critical location achieving its limit deformation. (Step 10 for DMPD is presented after step 14 below)

a) Calculate initial values $T_n^{\mathrm{i}_o=1}$ and $D_n^{\mathrm{i}_i=1}$

i. $D_1 = \frac{u_{r1lim}}{\Gamma_1 \phi_{r1}}$ (14)

where u_{r1lim} is the reference node translation, extracted from the 1st mode pushover analysis data, corresponding to the 1st time a deformation limit (drift or strain) is achieved. ϕ_{r1} is the value of the 1st mode shape translational term at the modal effective height h_1.

ii. Using $\mu_1 = \max\left(\frac{D_1}{D_{y1}}, 1\right)$ enter the constant $\mu = \mu_1, r = r_1$ design RS at D_1 to estimate $T_1^{\mathrm{i}_o=1}$ (initial elastic period) and calculate the corresponding higher mode periods $T_n^{\mathrm{i}_o=1} = \gamma_{Tn} T_1^{\mathrm{i}_o=1}$

iii. Using $\mu_n = \max\left(\frac{\gamma_{Tn} D_1}{D_{yn}}, 1\right)$ enter the constant $\mu = \mu_n$, $r = r_n$ design RS at $T_n^{\mathrm{i}_o=1}$ to estimate $D_n^{\mathrm{i}_i=1}$

b) Outer iteration loop: for i_o = 1, 2…

i. Inner iteration loop: for i_i = 1, 2…,
Compute $\mu_n^{i_i} = \frac{D_n^{i_i}}{D_{yn}}$, then retrieve $D_n^{i_i+1}$ from design RS using $T_n^{i_o}$ and $\mu_n^{i_i}$
Repeat step 10bi until $\max_{n=1:N}\left|1 - \frac{D_n^{i_i+1}}{D_n^{i_i}}\right|$ is acceptably close to zero.

ii. Estimate wall interstory drift responses: Extract the modal contributions to wall interstory drift responses from the pushover analysis results corresponding to $\boldsymbol{u_{rn}} = \Gamma_n \boldsymbol{\phi_{rn}} D_n^{i_i+1}$. Calculate total wall drifts $\boldsymbol{\theta_{j,i}^{i_o}}$ using an appropriate modal combination rule. Compare wall drifts to limits and compute drift performance indices:

$$dPI_{j,i}^{i_o} = \frac{\boldsymbol{\theta_{j,i}^{i_o}}}{\boldsymbol{\theta_{lim}}} - 1 \quad \text{and} \quad DPI^{i_o} = \max_{\mathrm{ji}}\left(dPI_{j,i}^{i_o}\right) \tag{15}$$

iii. Estimate wall curvature responses: There are a number of ways to estimate total curvature response. As the example presented in section 4 happens to be for low levels of ductility, having no yielding except at the wall bases, the same procedure was used for curvatures as was used for drifts. However, for higher levels of plastic rotation a more accurate estimation might be obtained by imposing the predicted total displacement vector (combined modal contributions extracted from pushover results corresponding to $\boldsymbol{u_{rn}} = \Gamma_n \boldsymbol{\Phi_{rn}} D_n^{i_i+1}$) on the MDF model in a nonlinear static analysis and using the predicted member end curvatures as the estimate (Reyes, 2012).

Extract the modal contributions to wall curvature responses (at member ends) from the pushover analysis results corresponding to $\boldsymbol{u_{rn}} = \Gamma_n \boldsymbol{\Phi_{rn}} D_n^{i_i+1}$. Calculate total member end curvatures $\boldsymbol{\varphi}^{i_o}_{\boldsymbol{j=1:2N_s,i=1:5}}$ using an appropriate modal combination rule. Compare wall curvatures to the strain based limits $\boldsymbol{\varphi}_{lsi}$ computed in step 3 and compute curvature performance indices:

$$cPI_{j,i}^{i_o} = \frac{\varphi_{j,i}^{i_o}}{\varphi_{lsi}} - 1 \quad \text{and} \quad CPI^{i_o} = \max_{\mathrm{ji}}\left(cPI_{j,i}^{i_o}\right) \tag{16}$$

iv. Compute the key performance index as

$$kpi^{i_o} = \max\left(DPI^{i_o}, CPI^{i_o}\right) \tag{17}$$

v. If any of the predicted peak wall responses are unacceptably large or if the key performance index kpi^{i_o} is too low, adjust the periods of the SDF systems using Eq. (18):

$$T_1^{i_o+1} = T_1^{i_o}\left(\frac{1}{kpi^{i_o}}\right)^P \quad \text{and} \quad T_n^{i_o+1} = \gamma_{Tn} T_1^{i_o+1} \tag{18}$$

where $P \approx 1$ is a parameter controlling convergence. Increase i_o by one, let $D_n^{i_i} = D_n^{i_i+1}$ and repeat step 10b until the critical location's deformation is acceptably close to its limit. When convergence is achieved compute final values as $T_n = T_n^{i_o+1}$ and $D_n = D_n^{i_i+1}$.

11) Scale strengths and stiffnesses to match the design $\boldsymbol{T_1}$.

$$M_{yj,i} = F_k M'_{yj,i} \text{ and } EI_{j,i} = F_k EI'_{j,i} \text{ where } F_k = \left(\frac{T'_1}{T_1}\right)^2 \tag{23}$$

12) Compute design moments considering geometrical nonlinearity (PΔ effects).

Multiply $M_{yj,i}$ by $F_{P\Delta} = \left(EI_{1,1} + \frac{mgh_r^3}{13}\right)/EI_{1,1}$ where m is the seismic mass per m height ($m = m_1/h_s$ where m_1 is the story seismic mass and h_s is the story height) and g is gravity i.e. $M^*_{j,i} = F_{P\Delta} M_{yj,i}$. Longitudinal steel reinforcement may be designed using any standard codified section/member analysis method considering the design moment and axial force demands. If design code steel reinforcement ratio limits govern some sections the design engineer will have to judge how significantly the performance of the built structure will be affected and to what extent this needs to be accounted for in the design.

13) Compute design shears considering geometrical nonlinearity (PΔ effects).

To determine the design shear distribution, modal contributions to wall story shears $V'_{j,i,n}$ may be extracted from the push over results corresponding to the maximum values occurring from $\boldsymbol{u_{rn}} = 0\ to\ \Gamma_n \boldsymbol{\Phi_{rn}} D_n$ and multiplied by F_k. That is $V_{j,i,n} = F_k V'_{j,i,n}$. These contributions are combined using an appropriate modal combination rule to determine $V_{j,i}$. $V_{j,i}$ should then be multiplied by $F_{P\Delta}$ to consider PΔ effects. The resulting shear distribution should be adjusted, if necessary, to ensure that the shear capacity of each story equals at least that of the story above it. This determines the raw design shear demand distribution $V_{j,i}^{raw}$ up the height of each wall i.e. $V_{j,i}^{raw} = F_{P\Delta} V_{j,i} \geq V_{j+1,i}^{raw}$. The sum of the overstrength moment capacities at each end of a member divided by the member length provides an upper bound on the member's shear demand.

These design capacities for intended plastic hinge and elastic regions include consideration of capacity design principles for nonlinear and dynamic higher mode effects. Note that in the generation of the raw design shears no empirical factors were required to account for dynamic amplification. These raw design shears must be increased at least by a material overstrength factor relating to the flexural reinforcement and a factor of safety accounting for possible variance of actual material strengths compared to nominal design strengths.

Steel reinforcement for shear may then be designed using any standard codified section/member analysis method considering the design shear, moment and axial forces. If desired, the design base shear demand may be computed from $V_b = \sum_{i=1}^{nz} V_{1,i}^{raw}$ where nz is the number of walls in the direction of the ground motion.

14) Repeat steps 2-13 for all other relevant limit states which may govern the design

Step 10 for Direct Modal Pushover Design

10) Estimate the $\mathbf{T_1}$ corresponding to the critical location achieving its design deformation.

a) Estimate roof yield and limit displacements, $u_{ryi} = \frac{\varphi_{yi} {h_r}^2}{3}$ and $u_{rdi} = u_{ryi} + h_r \theta_{p,i}$ respectively, allowable ductilities, $\mu_i = u_{rdi}/u_{ryi}$, and strain based rotation limits for plastic hinges, $\theta_{plsi} = L_{pi}(\varphi_{lsi} - \varphi_{yi})$, for all walls. If $\theta_{p,i} = \theta_{plsi}$ then strain governs the design roof displacement of the i^th wall.

b) Estimate relative plastic hinge secant rotational stiffnesses to peak ductility.

Insert rotational springs at locations of intended plastic hinges. The stiffnesses of these springs represent secant moment-plastic rotation stiffness to an estimated peak ductility response. The peak wall ductilities, $\mu_i^* \geq 1$, may be estimated by scaling the 1st mode shape so that the critical wall reaches its limit displacement u_{rdi}. The associated plastic hinge rotations may be computed using Eq. (19):

$$\theta_{pi}^* = \frac{u_{ryi}}{h_r}(\mu_i^* - 1) \tag{19}$$

The secant stiffness of the rotating plastic hinges, having $\theta^*_{pi} > 0$, are then estimated using Eq. (20)

$$k'_{\theta i} = \frac{M'_{y1,i}}{\theta^*_{pi}}\left(1 + \frac{\mathrm{r}h_r}{3L_{pi}}(\mu^*_i - 1)\right) \tag{20}$$

where r is the post yield to elastic flexural stiffness ratio of the bilinear approximation of the moment – curvature relation of the wall plastic hinges.

c) Form relative secant stiffness matrix $\mathbf{K_{sec}}$ using $k'_{\theta i}$ and $EI'_{j,i}$ and compute modal terms $\boldsymbol{\phi_{en}}$ and Γ_{en} where the subscript 'e' refers to „effective' stiffness. This process is similar to computing the elastic modal properties in step 6 except rotational springs having stiffnesses $k'_{\theta i}$ are included in the characterization of the structural stiffness.

d) Estimate the ratio of modal spectral displacement demands $\gamma_{Dn} = D_n/D_1$.

   i. Estimate limit displacement D_1 using Eq. (14) with Γ_{e1} and ϕ_{re1} instead of Γ_1 and ϕ_{r1} respectively.

   ii. Using $\mu_1 = \frac{D_1}{D_{y1}}$ enter the constant $\mu = \mu_1, r = r_1$ design RS at D_1 to estimate T_1 (initial elastic period) and calculate the corresponding higher mode periods $T_n = \gamma_{Tn} T_1$.

   iii. Using $\mu_n = \frac{\gamma_{Tn} D_1}{D_{yn}}$ enter the constant $\mu = \mu_n$, $r = r_n$ design RS at T_n to estimate D_n.

   iv. Let $\gamma_{Dn} = D_n/D_1$.

e) Calculate the design 1st mode spectral displacement D_1 considering higher mode effects. If drift governs the design roof displacement of the critical wall (see step 10a) then D_1 is computed using the minimum value for all stories of all walls of the following values computed for the drift limit.

$$D_1 = D_{1\Delta} = \min_{i=1:N_w, j=1:N_s}\left(\frac{\Delta_{lim} sh}{\sqrt{\sum_{n=1}^{N}\left(\Gamma_{en}\left(\boldsymbol{a_{wij}\phi_{en}} - \boldsymbol{a_{wij-1}\phi_{en}}\right)\gamma_{Dn}\right)^2}}\right) \tag{21}$$

where Δ_{lim} is the drift limit.

However, if strain governs the design roof displacement of the critical wall then D_1 is computed using the minimum value for all walls of the following values computed for the material strain limits indicated by plastic hinge rotations:

$$D_1 = D_{1\varepsilon} = \min_{i=1:N_w}\left(\frac{\theta_{plsi}}{\sqrt{\sum_{n=1}^{N}(\boldsymbol{a_{wi}}\Gamma_{en}\boldsymbol{\phi_{en}}\gamma_{Dn})^2}}\right) \tag{22}$$

where θ_{plsi} is the plastic rotation, computed in step 10a, of the intended plastic hinge at the base of the ith wall corresponding to the material strain limit.

f) Repeat steps d) ii-iii once using γ_{Dn} instead of γ_{Tn} in step iii to find T_n, μ_n and D_n

4. EXAMPLE: 8 Story One Way Asymmetric Plan RC Wall Structure

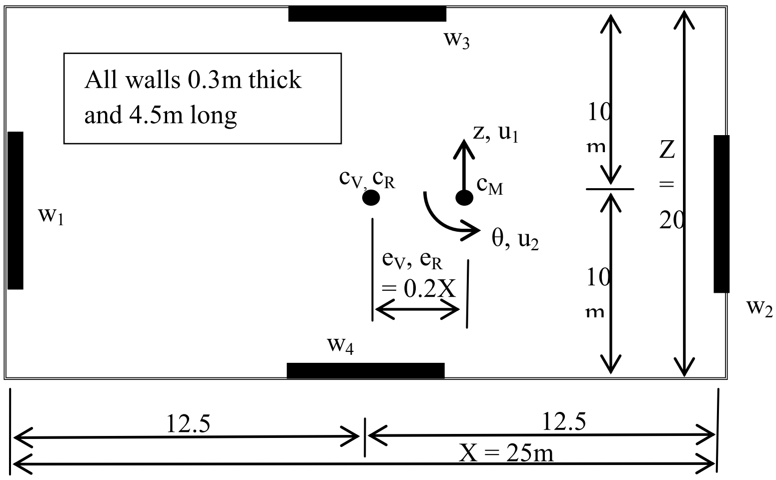

Figure 1. Plan of example 8 story 1 way asymmetric plan RC wall structure

MPD and DMPD designs were generated for a 8 story one way asymmetric plan wall structure having the plan geometry shown in Fig. 1 below (gravity frames, stair well etc. not shown). Plan asymmetry was accomplished by considering a center of mass, c_M, 0.2X to the right of the center of resistance, c_V and c_R. A symmetric stiffness system with mass eccentricity was used to test the methodology. However, another common case would have the center of mass located at the geometric center of the floor slabs with walls of unequal length.

The designs were verified using twenty ground motions from the LA10in50 ensemble scaled using a computer program called SeismoMatch (Seismosoft, 2010) to match their RS to the elastic design spectrum which had a corner period of 4s, a corner spectral displacement of 0.6m and a spectral acceleration plateau at 1g. The ground motion was applied in the z direction. Ground motion number 20 caused collapse of the MPD design during the NTHA verification and these results were excluded from the computation of the mean peak responses shown in figures 2 - 4.

Lumped mass models consisting of beam-column line elements having potential plastic hinges at each end were analyzed using the large displacement formulation option with the Newmark average acceleration numerical solution scheme in RUAUMOKO3D (Carr, 2006). Rigid floor diaphragms were assumed and the plastic hinges were assigned the modified Takeda hysteresis model with parameter values 0.25, 0.3, 1.0 and for α, β and the reloading stiffness power factor respectively. Unloading was „as in DRAIN-2D'. P-Delta effects were modeled by assigning the walls axial loads from realistic tributary floor areas and employing a P-Delta gravity column located at the c_M having pinned ends to carry the rest of the floor weight. The walls carried 38% of the gravity loads directly and gravity column the other 62%.

Relative flexural strength was distributed according to step 4 of the detailed step by step procedure outline in section 3.4.2. Relative target proportions of 1 and 0.5 were specified for the 1st story and top story moment capacities respectively, with a constant capacity from the top of the intended plastic hinge zones up to around 75% of the building height. The plastic hinge zones had relative flexural capacities equal to 80% of those in the 1st story. This may not comply with the moment capacity envelope requirements of some seismic design codes. The resulting strength eccentricity was -0.2X and the stiffness eccentricity was also -0.2X.

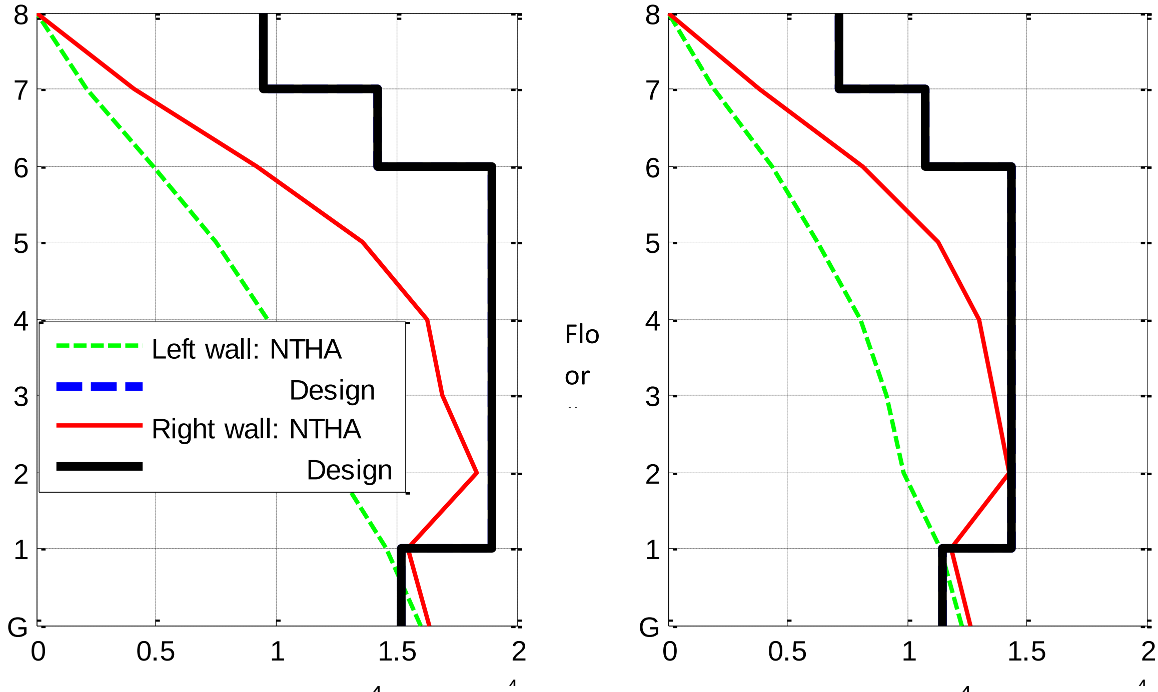

(a) DMPD V (x10^{4}kNm) (b) MPD V (x10^{4}kNm)

Figure 2. Design moment capacities Vs mean peak story moments

It can be seen from Fig. 2 that the right wall experienced significantly higher mean peak moment demands than the left wall. This is expected from static considerations of the lateral load resisting system and the fact that the effective inertia loads would be applied at the c_M which is much closer to the right wall.

Mean peak interstory drift ratios at the outer edges of the slab are compared to the deformation limits in Fig. 3(a). The drift in the top story at the right edge of the floor slab governed both designs. It can be seen that the DMPD generated a more conservative design in this case. The DMPD design required 45% more longitudinal steel than the MPD design but only achieved a maximum mean peak drift of 1.88% of the 3m story height, which is 6% less than the limit. The MPD design overshot the drift limit by 8.7% of the story height. However, as it required much less steel, this design could still be more attractive to some building owners.

Mean peak curvature responses are shown in Fig. 3(b) below. The influence of the 25% increase of flexural capacity at the top of the intended plastic hinge regions at the 1st floor is clear. It is more likely that the moment capacity would change within the 2nd story, where the longitudinal steel reinforcement would probably be curtailed, than at the 1st floor level as shown in Fig. 2. As drift governed, the mean peak curvatures were all below values corresponding to the strain limits. The largest ratio of demand/limit was approximately 0.88 at the bottom of the right wall for the MPD design and 0.73 at the same location for DMPD. For DMPD the maximum mean peak curvature ductilities were around 9 at the bottom of the right edge wall and around 10 at the same location for MPD. From the curvature ductility in Fig. 3(b) results it can be seen that significant yielding was effectively limited, almost completely, to the ground story by the relative vertical strength distribution selected in step 4.

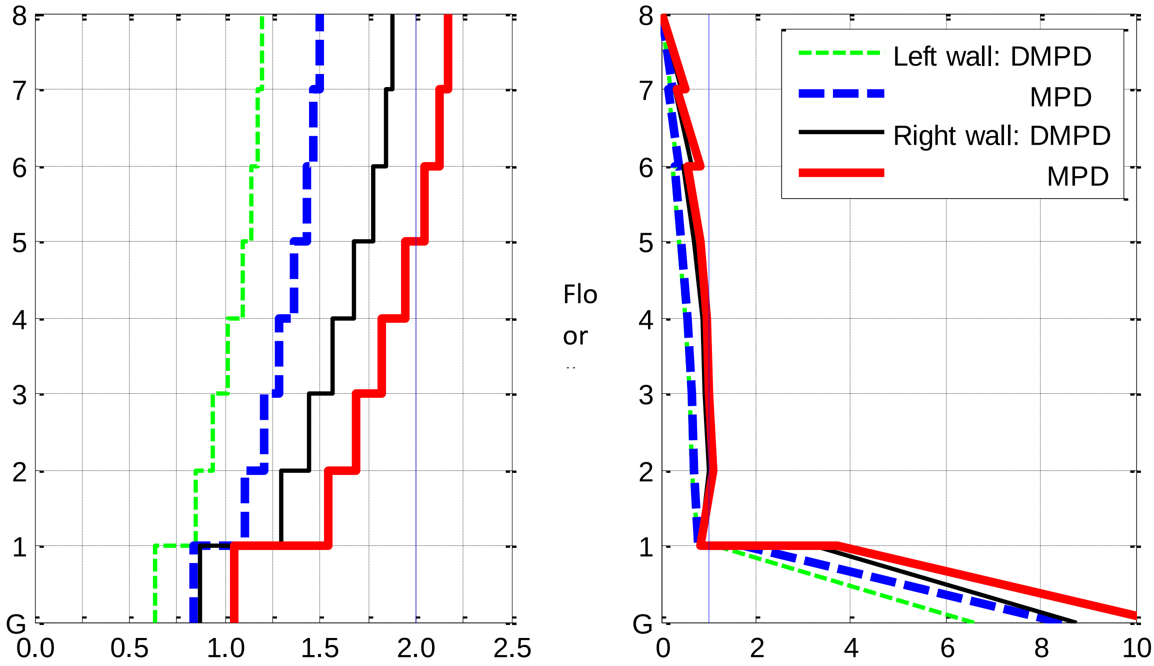

(a) Mean peak drifts (%) at edge walls (b) Mean peak curvature ductilities

Figure 3. Drift and curvature response

Fig. 4 below shows the raw design shear distributions generated by DMPD and MPD verses the mean peak NDA results from the verification analyses. The raw shears are the direct output from the procedure and have not had any empirical factors applied to them. Both ductility and higher mode effects were considered in the determination of these raw shears. Traditional dynamic amplification factors are therefore not required when MDBD is used to compute seismic design actions.

7 modes had modal effective masses greater than 1% of the total seismic mass and so were considered in the estimations of peak responses. Higher modes contributed significantly to moment demand in the upper stories but especially to shear forces (shown in Fig. 4 below). Both the DMPD and MPD design shears provide capacity envelopes comfortably exceeding the verified mean peak demands in the upper stories. However, some of the raw design shears are less than the verified mean peak demands in the lower two stories. Therefore it is clear that increasing these raw shears by material overstrength factors and safety factors to account for material variability would be advisable.

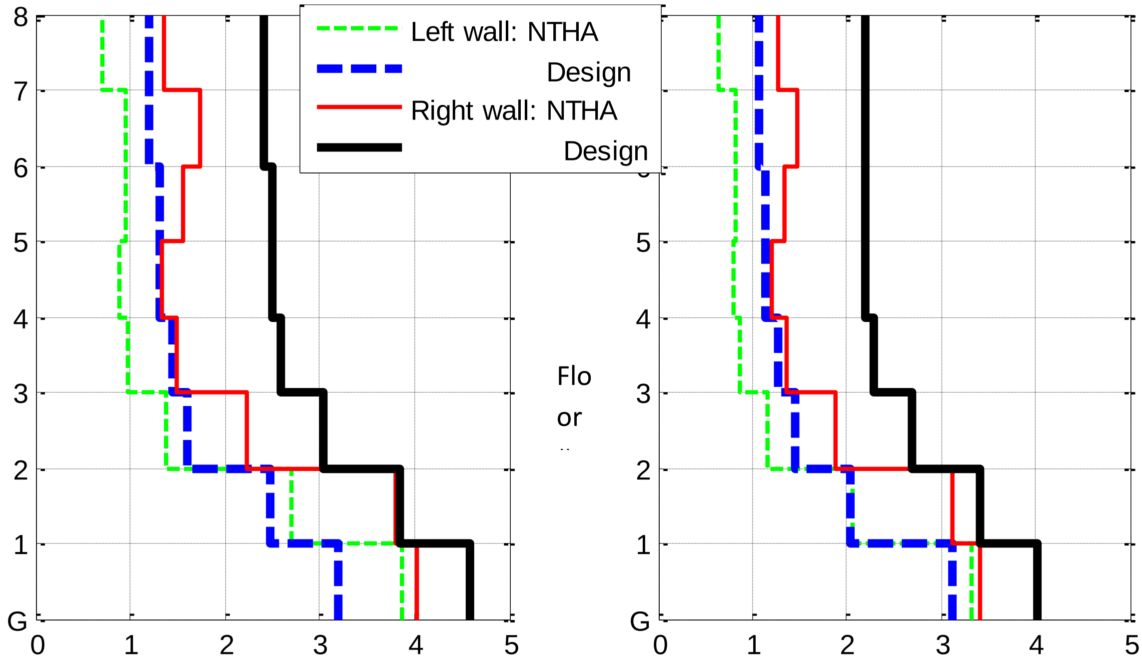

(a) DMPD V (MN) (b) MPD V (MN)

Figure 4. „Raw' design shears Vs mean peak story shears

5. CONCLUSIONS

The Modal Displacement Based Design method was extended to multistory one way asymmetric plan RC wall structures and results presented for an 8 story mass eccentric wall structure. Both MPD and DMPD were found to generate designs which achieved mean peak critical responses within 10% below to 10% above the governing drift limit. The methods were also found to generate raw design shear actions which reflected ductility and dynamic higher mode effects. There was an adequate match between the design shear values and the NTHA verification results although in the lower two stories some of the raw shears were less than the NTHA results. It was recommended that the raw shear actions be increased, at least by a suitable overstrength factor for the longitudinal flexural reinforcing steel and a safety factor accounting for possible variation of the material strengths from the values used in the design.

Advantages of MDBD include direct consideration of nonlinear behaviour including ductility and PΔ effects, and dynamic higher mode effects in the design procedure. Capacity design principles can also be included at the start of the design process enabling explicit determination of design shear and flexural capacity distributions. DMPD has the additional advantage of being direct not iterative.

ACKNOWLEDGEMENTS

Support for this work was provided by the Ministry of Housing and Construction of Israel through the National Building Research Institute of the Department of Civil and

Environmental Engineering at the Technion. The authors gratefully acknowledge this support.

REFERENCES

Alvarez, B.J.C., (2004), *Displacement-based design of continuous concrete bridges under transverse seismic excitation.* Masters dissertation, European school for advanced studies in reduction of seismic risk (ROSE School), University of Pavia, Italy

Beyer, K.,Dazio, A., Priestley, M.J.N., (2008), *Seismic design of torsionally eccentric buildings with RC U-shaped walls*, Research Report No. ROSE-2008/03, Rose School, IUSS Press, Pavia, 303 pp

Carr AJ (2006) RUAUMOKO – Program for inelastic dynamic analysis. Department of Civil Engineering, University of Canterbury, Christchurch.

Castillo, R., (2004), *Seismic Design of Asymmetric Ductile Systems*, PhD Thesis, University of Canterbury, Christchurch, New Zealand

Chopra, A.K., Goel, R.K., (2002), "A modal pushover analysis procedure for estimating seismic demands for buildings", *Earthquake Engineering and Structural Dynamics,* Vol.31(3), pp. 561–582

Chopra, A.K., (2007), *Dynamics of Structures: Theory and Applications to Earthquake Engineering, Third Edition,* Prentice Hall, New Jersey

Drain-2D**,** *a general-purpose computer program for dynamic analysis of inelastic plane structures, Report no. EERC 73-6*

Goel, R. R. and Chopra, A. K. (2005), "Extension of Modal Pushover Analysis to Compute Member Forces", *Earthquake Spectra*, 21, pp. 125-140.

Kowalsky, M.J., (2002), "A displacement-based approach for the seismic design of continuous concrete bridges", *Earthquake Engineering & Structural Dynamics*, Vol. 31, pp. 719–747, doi: 10.1002/eqe.150

Priestley, M.J.N., Calvi, G.M., Kowalsky, M.J., (2007), *Displacement-Based Seismic Design of Structures*, IUSS Press, Pavia, 721pp

Seismosoft, (2010), SeismoMatch (version 1.3.0. Build 101): A computer program for spectrum matching of accelerograms. Available at: http://www.seismosoft.com/

Wilkinson, P.J., Lavan, O., Rutenberg, A.V., (2012), "Modal Displacement Based Seismic Design of Asymmetric-Plan Structures", Proceedings of the 15th World Conference on Earthquake Engineering, 24-28 September 2012, Lisbon, Portugal

Wilkinson, P.J. and Lavan, O., (2013), "Modal Displacement Based seismic Design of multi-story one way asymmetric plan building structures", Proceedings of the Structures Congress, 2-4 May 2013, Pittsburgh, Pennsylvania, United States of America